Anal. Chem. **2000,** *72,* 3122−3128

Imaging Size-Selective Permeation through Micropatterned Thin Films Using Scanning Electrochemical Microscopy

Mary Elizabeth Williams, Keith J. Stevenson, Aaron M. Massari, and Joseph T. Hupp*

Department of Chemistry, Northwestern University, Evanston, Illinois 60208

This paper describes a new approach for quantification of rates of molecular transport through patterned, or otherwise heterogeneous, porous films supported on conductive substrates. Scanning Electrochemical Microscopy (SECM) has been used to image molecular sieving of redox active probes by thin, electropolymerized films of Fe(5-amino-1,10-phenanthroline)$_3^{2+}$ on micropatterned and microdisk array electrodes. Films as thin as 12 nm completely block redox mediators with average molecular diameters greater than 12 Å, whereas smaller diameter probes (radii 5−8 Å) were observed to permeate selectively. SECM tip currents measured for three different redox permeants/mediators are observed to decrease with increasing polymer thickness, consistent with a transport model that includes partitioning into and diffusion within the polymer films. Permeabilities, PD_f, within the poly-[Fe(5-NH$_2$-phen)$_3^{2+}$] films have been quantitatively determined from the SECM tip currents and are in excellent agreement with data previously obtained from rotating-disk electrochemistry. This new methodology provides a versatile approach for quantitative investigation of membrane transport and permeation selectivity with good lateral spatial resolution.

The rational design and preparation of mesoporous materials that demonstrate size- and chemo-selective transport is of particular technological significance and economic importance in the contexts of catalysis,[1] separations,[2] and chemical sensing.[3] Available methods for investigation of transport selectivity of membrane and thin-film materials include, for example, quartz crystal microgravimetry (QCM),[4] rotating-disk electrochemistry (RDE),[5] and two-compartment diffusion cells.[6] While these techniques provide useful quantitative information, they generally measure bulk membrane transport properties and therefore represent ensemble-averaged molecular transport. It is therefore difficult to distinguish or measure individual component contributions arising from heterogeneous membrane composition (e.g., pinholes; cracks; and variations in crystallinity, thickness, and interface roughness).

Scanning electrochemical microscopy (SECM) has recently emerged as a powerful technique for investigation of mass transport, combining high-resolution visualization of surface topography with interfacial chemical and electrochemical reactivity information.[7] SECM has been used to study mass transport across synthetic[8] and biological membranes[9] and biomaterials;[10] ion transport and charge transfer within polymer films[11] and gels;[12] and mass transport across liquid/liquid interfaces.[13] The kinetics and thermodynamics of solute partitioning at the interface of two-phase systems have been analyzed as a function of SECM tip/

(1) For example: (a) Buttry, D. A.; Anson, F. C. *J. Am. Chem. Soc.* **1984**, *106*, 59. (b) Gaudalupe, A. R.; Usifer, D. A.; Potts, K. T.; Hurrell, H. C.; Mogstad, A. E.; Abruna, H. D. *J. Am. Chem. Soc.* **1988**, *110*, 3462. (c) Andrieux, C. P.; Haas, O.; Saveant, J. M. *J. Am. Chem. Soc.* **1986**, *108*, 8175.

(2) Recent examples include: (a) Jirage, K. B.; Hulteen, J. C.; Martin, C. R. *Science (Washington, D.C.)* **1997**, *278*, 655. (b) Hulteen, J. C.; Jirage, K. B.; Martin, C. R. *J. Am. Chem. Soc.* **1998**, *120*, 6603. (c) Jirage, K. B.; Hulteen, J. C.; Martin, C. R. *Anal. Chem.* **1999**, *71*, 4913.

(3) For example: (a) Frew, J. E.; Hill, H. A. O. *Anal. Chem.* **1987**, *59*, 933A. (b) Amos, L. J.; Duggal, A.; Mirsky, E. J.; Ragonesi, P.; Bocarsly, A. B. *Anal. Chem.* **1988**, *60*, 245. (c) Heller, A. *J. Phys. Chem.* **1992**, *96*, 3579. (d) Natan, M. J.; Wrighton, M. S. *Prog. Inorg. Chem.* **1989**, *37*, 391.

(4) For example: (a) Caruso, F.; Niikura, K.; Furlong, D. N.; Okahata, Y. *Langmuir* **1997**, *13*, 3427. (b) Juttner, K.; Ehrenbeck, C. *J. Solid State Electrochem.* **1998**, *2*, 60. (c) Moylan, C. R.; Best, M. E.; Ree, M. *J. Polym. Sci., Part B: Polym. Phys.* **1991**, *29*, 87.

(5) (a) Ikeda, T.; Schmehl, R.; Denisevich, P.; Willman, K.; Murray, R. W. *J. Am. Chem. Soc.* **1982**, *104*, 2683. (b) Leddy, J.; Bard, A. J. *J. Electroanal. Chem.* **1983**, *153*, 223. (c) Centonze, D.; Malitesta, C.; Plamisano, F.; Zambonin, P. G. *Electroanalysis* **1994**, *6*, 423.

(6) (a) Tercier, M. L.; Buffle, J. *Anal. Chem.* **1996**, *68*, 3670. (b) Park, I. S.; Do, D. D.; Rodrigues, A. E. *Catal. Rev.—Sci. Eng.* **1996**, *38*, 189.

(7) For example: (a) Bard, A. J.; Denuault, G.; Lee, C.; Mandler, D.; Wipf, D. O. *Acc. Chem. Res.* **1990**, *23*, 357. (b) Bard, A. J.; Fan, F.-R. F.; Mirkin, M. V. In *Electroanalytical Chemistry*; Bard, A. J., Ed.; Marcel Dekker: New York, 1994; Vol. 18, p 243. (c) Barker, A. L.; Gonsalves, M.; Macpherson, J. V.; Slevin, C. J.; Unwin, P. R. *Anal. Chim. Acta* **1999**, *385*, 223. (d) Bath, B. D.; White, H. S.; Scott, E. R. In *Scanning Electrochemical Microscopy*; Bard, A. J., Mirkin, M. V., Eds.; John Wiley & Sons: New York, in press.

(8) (a) Scott, E. R.; White, H. S.; Phipps, J. B. *J. Membr. Sci.* **1991**, *58*, 71. (b) Scott, E. R.; White, H. S.; Phipps, J. B. *Anal. Chem.* **1993**, *65*, 1537. (c) Bath, B. D.; Lee, R. D.; White, H. S.; Scott, E. R. *Anal. Chem.* **1998**, *70*, 1047.

(9) (a) Matsue, T.; Shiku, H.; Yamada, H.; Uchida, I. *J. Phys. Chem.* **1994**, *98*, 11001. (b) Yasukawa, T.; Uchida, I.; Matsue, T. *Biochim. Biophys. Acta* **1998**, *1369*, 152. (c) Scott, E. R.; White, H. S.; Phipps, J. B. *Solid State Ionics* **1992**, *53−56*, 176. (d) Scott, E. R.; Laplaza, A. I.; White, H. S.; Phipps, J. B. *Pharm. Res.* **1993**, *10*, 1699. (e) Scott, E. R.; Phipps, J. B.; White, H. S. *J. Invest. Dermatol.* **1995**, *104*, 142. (f) Tsionsky, M.; Zhou, J.; Amemiya, S.; Fan, F.-R. F.; Bard, A. J.; Dryfe, R. A. W. *Anal. Chem.* **1999**, *71*, 4300.

(10) (a) Macpherson, J. V.; Beeston, M. A.; Unwin, P. R.; Hughes, N. P.; Littlewood, D. *J. Chem. Soc., Faraday Trans.* **1995**, *91*, 1407. (b) Macpherson, J. V.; Beeston, M. A.; Unwin, P. R.; Hughes, N. P.; Littlewood, D. *Langmuir* **1995**, *11*, 3959. (c) Nugues, S.; Denuault, G. *J. Electroanal. Chem.* **1996**, *408*, 125. (d) Macpherson, J. V.; O'Hare, D.; Unwin, P. R.; Winlove, C. P. *Biophys. J.* **1997**, *73*, 2771.

10.1021/ac9914622 CCC: $19.00
Published on Web 06/10/2000

substrate separation and current−time transients.[14] Because each selected molecular probe has its own characteristic redox potential, SECM has the ability to differentiate individual fluxes of different analytes in a multicomponent solution.

We have become interested in development of experimental methods for investigation of ion and molecular transport through nanostructured, mesoporous materials. Of particular interest is the examination of size-selective transport through films of transition metal containing cyclophanes (molecular squares[15] and rectangles[16]) and electrodeposited polymer films.[17] Our initial studies of these polymer films,[17] and earlier studies by Murray et al.,[18] showed (via rotating-disk voltammetry measurements involving redox-active probe molecules) that electropolymerized films of $Fe(5\text{-}NH_2\text{-}phen)_3^{2+}$ possess nearly perfect molecular sieving properties, and are permeable to solutes with diameters less than ~12 Å. We have a particular interest in acquiring the ability to measure permeant transport rates while spatially differentiating between heterogeneous membrane/film regions or morphologies on surfaces.

We have therefore initiated SECM imaging of molecular transport in polymerized [$Fe(5\text{-}NH_2phen)_3^{2+}$] films as a well-characterized model system for development and application of SECM methods for investigating transport through films of mesoporous *molecular* materials. This paper describes the approach used to image molecular sieving qualitatively and to determine film permeation rates quantitatively within the polymer films using an SECM methodology.

EXPERIMENTAL SECTION

Chemicals. Iron(II) tris(5-amino-1,10-phenanthroline) hexafluorophosphate (denoted $Fe(5\text{-}NH_2\text{-}phen)_3^{2+}$) was prepared according to standard methods,[19] using 5-amino-1,10-phenanthroline ligand purchased from Polysciences, Inc. Aqueous solutions were prepared using ultrapure (18 MΩ cm) water (Barnstead Millipore). All other chemicals were used as received.

Instrumentation. Scanning electrochemical microscopy was performed with a CH Instruments model 900 SECM. All voltammetry and SECM measurements were performed in aqueous solutions using a Pt counter electrode and an Ag/AgCl reference electrode. The SECM tip position was visually observed with a CCD camera (Panasonic KR222, Edmund Scientific) and a video monitor. Prior to all SECM scans, the potentials of the tip and substrate were held for a minimum of 60 s.

Atomic force microscopy (AFM) was performed using a Digital Instruments Multimode Nanoscope IIIa. All measurements were obtained in tapping mode using single etched silicon (TESP) Nanoprobe SPM tips (cantilever length 125 μm and resonance frequency 307−367 Hz, Digital Instruments). Thickness measurements of the polymer films on ITO were obtained using the "section" analysis feature of the Digital Nanoscope software (version 4.23r2).

Preparation of Substrates and Electrodes. Indium tin-oxide (ITO) coated glass slides (Delta Technologies) were cleaned by soaking in a 20/80 (V/V) ethanolamine/water solution at 80 °C for 15 min, followed by sonication and rinsing with water. Micropatterned ITO substrates were prepared by spin coating photoresist (Shipley 1822) onto precleaned ITO slides at a spinning rate of 4000 rpm for 50 s, dried at 90 °C for 30 min, followed by rinsing with chlorobenzene. The photoresist-coated substrates were then placed in a Quintel Q-2001CT mask aligner, exposed for 50 s through a 50 μm × 50 μm grid, and immediately developed in a 1:1 dilution of Shipley Microposit developer and water.

In addition, a microdisk array, consisting of the exposed tips of six individual 25-μm-diameter Pt wires (Goodfellow) sealed in glass and contained within a single 1-cm-diameter epoxy (Shell Epon 828 Resin, Miller-Stephenson) cylinder, was constructed.[20] The microdisk array cylinder was machined, to expose the microelectrodes in a flat surface, and then polished with successively finer grades of alumina (to 0.03 μm, Buehler). The microelectrode areas were determined from limiting currents obtained during reductive scans in aqueous solutions of 5 mM $[Ru(NH_3)_6]Cl_3$ using standard methods.[21]

SECM tips consisting of 8-μm diameter carbon fibers (Alfa Aesar) were electrically connected to tungsten wires using conductive silver epoxy (Grace) and sealed in glass microcapillaries using a fast curing, insulating epoxy (ITWDevcon, Danvers, MA). The exposed carbon fiber was insulated by electrodeposition of poly(oxyphenylene) according to literature methods.[22] The tip of the carbon fiber was freshly exposed using a sharp blade prior to each experiment; and the area of the carbon fiber disk electrode was determined from cyclic voltammetry limiting currents, as described above.

Preparation of Electropolymerized Films. Polymer films were formed during cycling of the electrical potential of the supporting platform in aqueous solutions containing 0.5 mM $Fe(5\text{-}NH_2phen)_3^{2+}$ as described previously.[17] The coated platforms

(11) (a) Kwak, J.; Anson, F. C. *Anal. Chem.* **1992**, *64*, 250. (b) Lee, C.; Anson, F. C. *Anal. Chem.* **1992**, *64*, 528. (c) Jeon, I. C.; Anson, F. C. *Anal. Chem.* **1992**, *64*, 2021. (d) Troise Frank, M. H.; Denuault, G. *J. Electroanal. Chem.* **1994**, *379*, 399. (e) Troise Frank, M. H.; Denuault, G. *J. Electroanal. Chem.* **1993**, *354*, 331. (f) Tsionsky, M.; Bard, A. J.; Dini, D.; Decker, F. *Chem. Mater.* **1998**, *10*, 2120.

(12) (a) Pyo, M.; Bard, A. J. *Electrochim. Acta* **1997**, *42*, 3077. (b) Fan, F.-R. F. *J. Phys. Chem. B* **1998**, *102*, 9777.

(13) (a) Barker, A. L.; Unwin, P. R.; Amemiya, S.; Zhou, J.; Bard, A. J. *J. Phys. Chem. B* **1999**, *103*, 7260. (b) Shao, Y.; Mirkin, M. V. *J. Phys. Chem.* **1998**, *102*, 9915.

(14) Barker, A. L.; Macpherson, J. V.; Slevin, C. J.; Unwin, P. R. *J. Phys. Chem. B* **1998**, *102*, 1586.

(15) (a) Belanger, S.; Keefe, M. H.; Welch, J. L.; Hupp, J. T. *Coord. Chem. Rev.* **1999**, *192*, 29. (b) Belanger, S.; Hupp, J. T. *Angew. Chem., Int. Ed.* **1999**, *38*, 2222. (c) Belanger, S.; Hupp, J. T.; Stern, C. L.; Slone, R. V.; Watson, D. F.; Carrell, T. G. *J. Am. Chem. Soc.* **1999**, *121*, 557. (d) Slone, R. V.; Benkstein, K. D.; Belanger, S.; Hupp, J. T.; Guzei, I. A.; Rheingold, A. L. *Coord. Chem. Rev.* **1998**, *171*, 221.

(16) Benkstein, K. D.; Hupp, J. T.; Stern, C. L. *Angew. Chem., Int. Ed.*, in press.

(17) Belanger, S.; Stevenson, K. J.; Mudakha, S. A.; Hupp, J. T. *Langmuir* **1999**, *15*, 837.

(18) (a) Gough, D. A.; Leypoldt, J. K. *Anal. Chem.* **1979**, *51*, 439. (b) Presspich, K. A.; Maybury, S. G.; Thomas, R. E.; Linton, R. W.; Irene, E. A.; Murray, R. W. *J. Phys. Chem.* **1989**, *93*, 5568. (c) Ewing, A. G.; Feldman, B. J.; Murray, R. W. *J. Phys. Chem.* **1985**, *89*, 1263.

(19) Fussa-Rydel, O.; Zhang, H.-T.; Hupp, J. T.; Leidner, C. R. *Inorg. Chem.* **1989**, *28*, 1533.

(20) Wooster, T. T.; Longmire, M. L.; Zhang, H.; Watanabe, M.; Murray, R. W. *Anal. Chem.* **1992**, *64*, 1132.

(21) Wightman, R. M., Wipf, D. O. In *Electroanalytical Chemistry*; Bard, A. J., Ed.; Marcel Dekker: New York, 1980; Vol. 15.

(22) Potje-Kamloth, K.; Janata, J.; Josowicz, M. *Ber. Bunsen-Ges. Phys. Chem.* **1989**, *93*, 1480.

Scheme 1. Cartoon Comparing the Mass Transport during Rotating Disk Electrochemistry (left) and SECM (right) Experiments, Where O and R Represent the Oxidized and Reduced Forms of the Redox Probe, Respectively; D_s and D_f Are the Diffusion Coefficients in the Solution and Film, Respectively; *d* Is the Thickness of the Film[a]

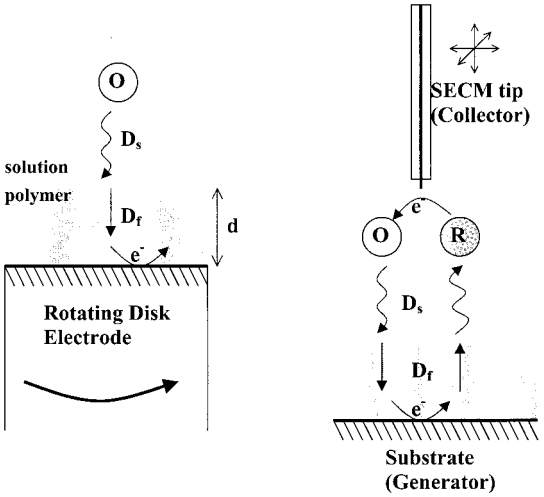

[a] The partition coefficent, *P*, for the analyte across the polymer/solution interface is not depicted

were removed from the polymerization solution and rinsed with copious amounts of water. AFM images of the electropolymerized films on ITO were obtained after removing the photoresist grid by rinsing with acetone.

RESULTS AND DISCUSSION

To develop new methods for the study of mass transport processes, it is first necessary to employ a model system. Our previous work[17] reported permeation rates obtained from RDE voltammetry through polymer films electropolymerized onto disk electrodes with large surface areas, >0.25 cm^2. We sought to utilize this information to develop a new SECM methodology for these measurements. A schematic of these two techniques is illustrated in Scheme 1. The left-hand side of Scheme 1 depicts the measurement of molecular transport to a rotating disk electrode through first the bulk solution and the polymer film. In comparison, SECM can be used to image mass transport *from* the conductive support surface, by positioning the SECM probe above the substrate (Scheme 1, right) and poising the potential to detect species diffusing from the film (e.g., the "collector"). The well-characterized electropolymerized films were chosen as a model system for development of SECM, with the goal of using these experiments in our studies of nanostructured molecular materials.[15,16]

Since the polymerized Fe(5-NH_2-phen)$_3^{2+}$ films were previously found to be amorphous and defect free,[17] imaging these surfaces by SECM would likely result in relatively nondescript current responses that would provide little additional information. Consequently, we prepared intentionally structured films by carrying out the Fe(5-NH_2-phen)$_3^{2+}$ polymerization on a micropatterned substrate featuring a known, regular array of conductive and insulating areas. The patterned films allow facile quantification of

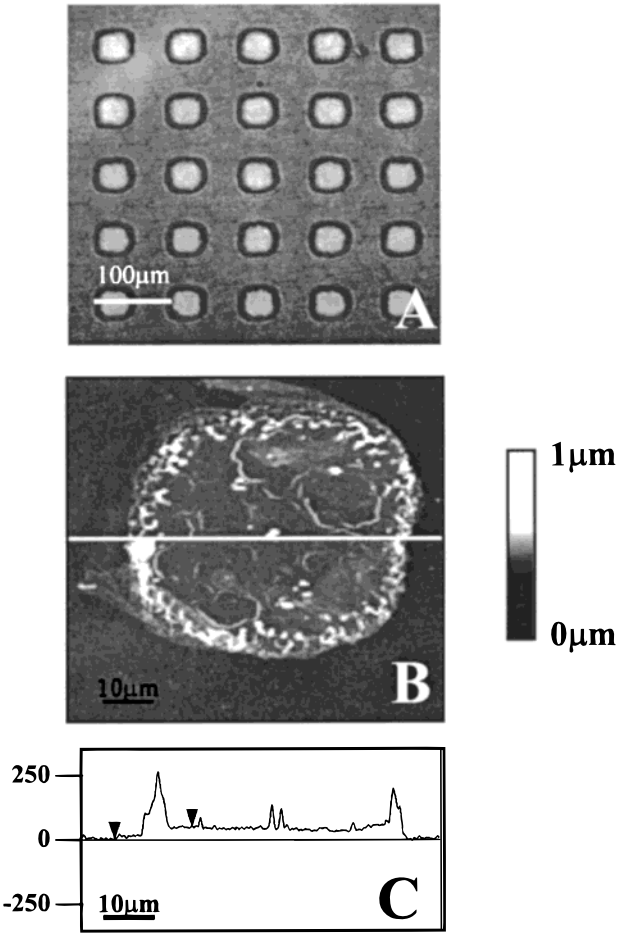

Figure 1. (A) Optical micrograph of a 500 μm × 500 μm area of ITO substrate with a photoresist pattern. (B) Tapping mode AFM image of a micropatterned electropolymerized poly(Fe(5-NH_2-phen)$_3^{2+}$) film, with (C) the image cross-section.

transport rates and also provide a means for locating specific target areas on the surface. In addition, the pattern serves as a reference registry for pre- and post-surface characterization by ex-situ methods (e.g., AFM, XPS, and EDX). The ITO support material can be used as the working electrode in the oxidation of Fe(5-NH_2phen)$_3^{2+}$ to form thin polymer films of controllable thickness within the patterned ITO holes. An optical micrograph of an ITO substrate, patterned with a photoresist mask using standard photolithographic methods, is shown in Figure 1A. The process produces a continuous array of evenly spaced 50 μm × 50 μm conductive microelectrodes (white squares in Figure 1A), separated by an insulating photoresist grid that is ~200 nm thick.

We have shown previously[17] that the extent of polymer film growth is a function of the number of applied anodic cycles, with the films reaching a self-limiting thickness, *d*, of ~50 nm. Figure 1B is a tapping-mode AFM image of one of the ITO squares coated with a poly[Fe(5-NH_2phen)$_3^{2+}$] film obtained after 100 voltammetric cycles. From the AFM image, the dimensions of the polymer-coated ITO hole are 48 μm × 46 μm and the surface of the polymer film is apparently amorphous and defect-free. The image cross-section (Figure 1C) reveals the average film thickness to be 51 nm, consistent with our earlier observations of polymer film growth on glassy carbon and ITO surfaces.[17]

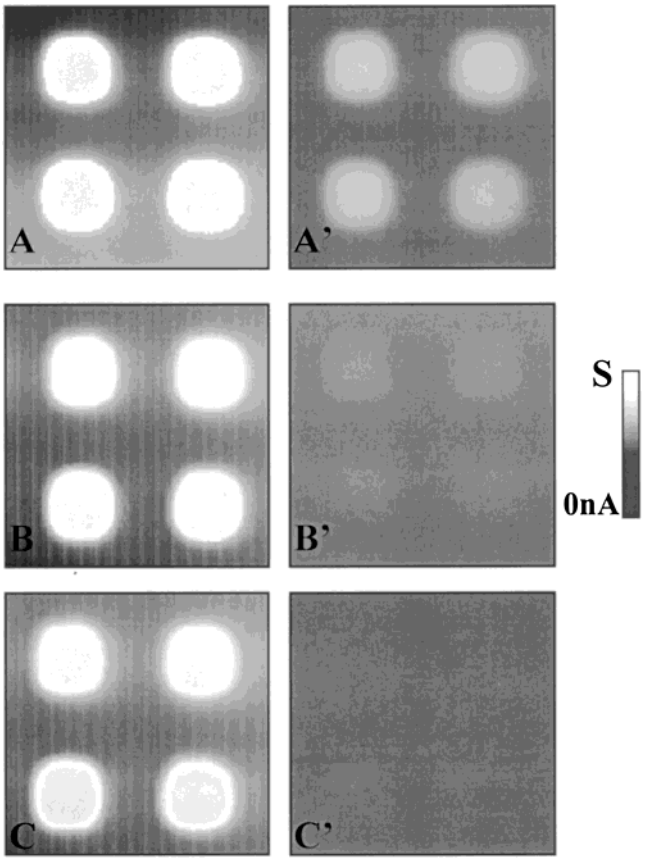

Figure 2. SECM images of a patterned array using a 4-μm radius carbon fiber tip held at 0 V (vs Ag/AgCl) scanning at a rate of 30 μm/s of (A, A′) 4.8 mM $[Ru(NH_3)_6]Cl_3$ and $E_{sub} = -0.35$ V; (B, B′) 5.1 mM $[Fe(phen)_3](SO_4)$ and $E_{sub} = +0.5$ V; (C, C′) 4.3 mM $Na_4[Fe(bphen(SO_3)_2)_3]$ and $E_{sub} = +1.0$ V. The images on the left (A, B, C) are scans of bare ITO patterned substrate. The right-hand images (A′, B′, C′) are images taken at the same tip−substrate separation distance (2 μm) as in (A, B, C), but the substrate is a ∼12-nm-thick film of electropolymerized Fe(5-NH_2-phen)$_3^{2+}$ on ITO. Current scales (*S*) are 4.3 nA for (A, A′); 7.1 nA (B, B′); and 1.2 nA (C, C′).

A SECM image of a micropatterned ITO substrate, obtained using the experimental approach depicted in the right-hand panel of Scheme 1, is shown in Figure 2A. In this experiment, the potential of the substrate (E_{sub}) is held at −0.35 V (vs Ag/AgCl), fully reducing $Ru(NH_3)_6^{3+}$ to $Ru(NH_3)_6^{2+}$ (i.e., the substrate is the "generator"), and the SECM tip is used to "sense" the amount of generated $Ru(NH_3)_6^{2+}$ using an applied potential (E_{tip}) of 0 V (i.e., the tip is the collector). The bright areas in the image indicate higher current at the SECM tip and correspond to the roughly 50 μm × 50 μm bare ITO holes. The photoresist layer is impermeable to $Ru(NH_3)_6^{3+}$ so that the tip current obtained above these areas is lower. The finite amount of current obtained above the photoresist layer is a result of the growth of the $Ru(NH_3)_6^{2+}$ diffusion layer from the bare ITO subtrate.[23] The currents observed in Figure 2A (and in other SECM images below) are independent of scan direction.

We have previously shown that the poly-[Fe(5-NH_2-phen)$_3^{2+}$] films possess the ability to exclude redox probes selectively on the basis of their size; we also observed that the permeation current for smaller probes decreased with increasing film thickness.[17] The films' selectivity implied the absence of large numbers of defect sites, but given the large area of the electrode surfaces in the RDE experiment, a direct relationship between microscale structure and transport behavior could not be derived. SECM is capable of simultaneously mapping both surface topography and probe permeation rates, and was thus used both to image selective permeation qualitatively and to assess the permeation rates within the films quantitatively.

Imaging Size-Selective Molecular Sieving. Figure 2 shows gray scale SECM images of an identical region of a patterned ITO substrate with bare ITO (A, B, C) or ITO with a 12-nm-thick poly-[Fe(5-NH_2phen)$_3^{2+}$] film (A′, B′, C′). The series of images was taken using aqueous solutions of three redox probes of varying diameters and charge: 5 mM $Ru(NH_3)_6^{3+}$, diameter 5.5 Å(A, A′); 5 mM $Fe(phen)_3^{2+}$, diameter 13 Å(B, B′); and 8 mM Fe(bathophenanthroline$(SO_3)_2)^{4-}$, diameter 24 Å(C, C′). In all six images, the SECM tip is maintained at constant height[24] and applied potential (0 V vs Ag/AgCl), acting as collector for the redox mediator which is electrogenerated at the substrate. Current is therefore only observed for species that permeate the polymer film.

Figure 2 parts A and A′ show that the SECM tip current obtained for the oxidation of $Ru(NH_3)_6^{2+}$ above the film-covered substrate (A′) is ∼25% lower than the current above bare ITO (A). Images (not shown) obtained with the redox mediators ferrocenemethanol (FcMeOH), ferricyanide, and ferrocyanide (with diameters 4.5, 6.0, and 6.0 Å, respectively) show similarly attenuated tip currents over polymer-covered substrates. In contrast, the redox mediators $Fe(phen)_3^{2+}$ and $Fe(bphen(SO_3)_2)_3^{4-}$ (Figure 2 parts B′, C′) have little or no observable tip permeation current (corresponding to the re-reduction of $Fe(phen)_3^{3+}$ and $Fe(bphen(SO_3)_2)_3^{3-}$, respectively) over the film-covered ITO. An identical effect is observed with $Co(phen)_3^{2+}$ (not shown). SECM images are readily obtained using these probes on bare ITO (Figure 2 parts B, C). The lack of signal observed for $Fe(phen)_3^{3+}$ and $Fe(bphen(SO_3)_2)_3^{3-}$ in the images of the film-covered substrate results from their exclusion from the polymer film on the basis of molecular size, where species with radii greater than 12 Å (Figure 2 parts B′,C′) are apparently completely blocked by the film, consistent with earlier reports.[17,18] The advantage of SECM is that we are simultaneously able to assess the film's spatial uniformity and size selectivity.

Quantification of Molecular Permeation Rates. The attenuation of the current response for $Ru(NH_3)_6^{2+}$ (as in Figure 2A′) results from the well-known contribution of permeation within the polymer film to the overall mass transport rate, where the total current at an electrode, i_{lim}^{∞}, may be expressed as[18]

$$\frac{1}{i_{lim}^{\infty}} = \frac{1}{i_{MT}} + \frac{1}{i_p} \qquad (1)$$

In eq 1, i_{MT} is the mass transport limited current for the electrode and i_P is the permeation current. Equation 1 was originally

(23) The details of the diffusion profiles above the pattern have not been extensively investigated, but are expected to be similar to observations made during SECM of porous membranes. See ref 7d.

(24) An approach curve is performed prior to only the first scan, so that the tip height above the substrate is ∼2 μm. Subsequent scans are performed at the same fixed height to eliminate distance effects from the analysis.

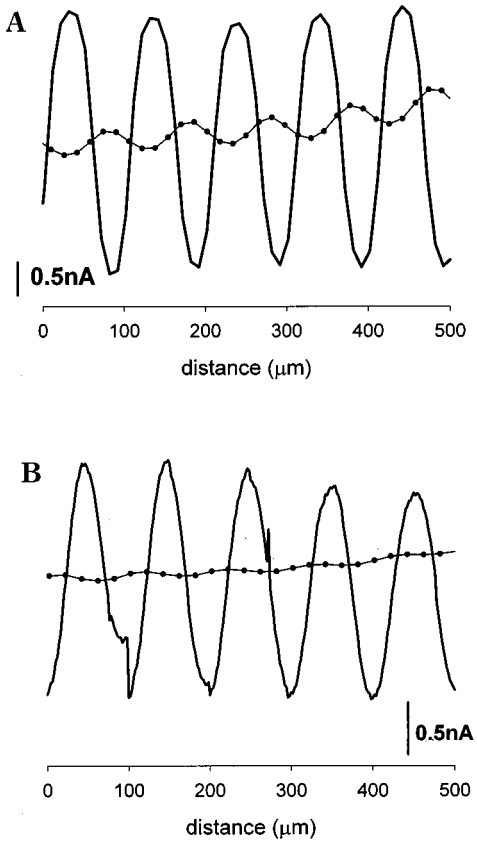

Figure 3. Current response as the SECM is scanned across the patterned array surface, in a 3 mM aqueous solution of FcMeOH, $E_{sub} = +0.5$ V and $E_{tip} = 0$ V (vs Ag/AgCl), for substrates with 12-nm- (A, -•-•-•-) or 38-nm-thick (B, -•-•-•-) metallopolymer films or over bare ITO (—). The tip currents scanning the polymer films (-•-•-•-) have been shifted on the current axis by +10 nA to overlay the response for the bare substrate (—).

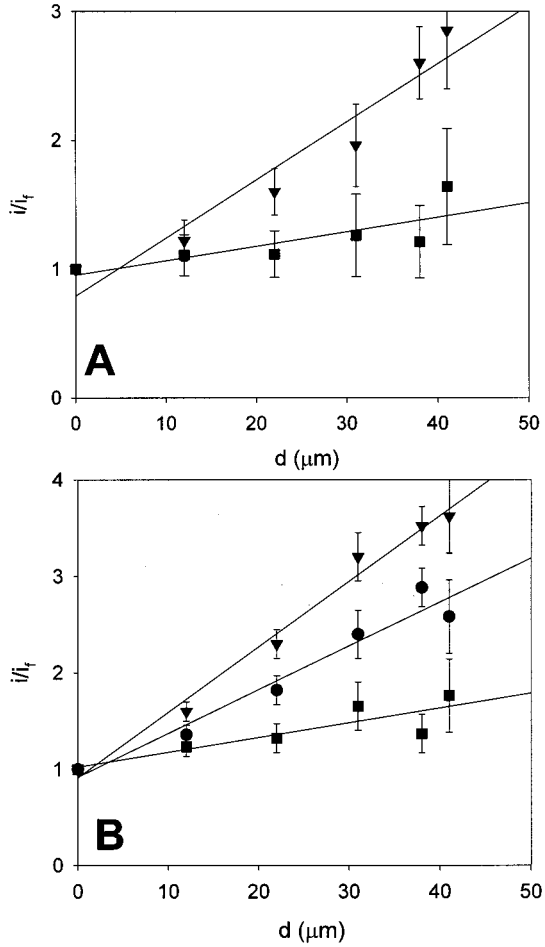

Figure 4. Plot of normalized tip current (i/i_f) versus polymer film thickness (d) for (A) the photoresist/ITO patterned substrate and (B) the Pt microdisk array of the redox mediators $Ru(NH_3)_6^{3+}$ (▼), $Fe(CN)_6^{4-}$ (●), and FcMeOH (■) using $E_{sub} = -0.35$, +0.4, and +0.35 V, respectively, and $E_{tip} = 0$ V vs Ag/AgCl.

developed for the limiting current measured using a film-covered electrode. For a microelectrode with radius r (i.e., a SECM tip), the current obtained at infinite distance from a bare substrate, i^∞ ($= i_{MT}$), is given by the well-known equation[25]

$$i^\infty = 4nFrD_sC \tag{2}$$

so that the limiting current in eq 1 is rewritten for a microdisk electrode measuring the diffusion of redox mediator at an infinite distance away from a film-covered substrate[18]

$$\frac{1}{i_f^\infty} = \frac{1}{4nFrD_sC} + \frac{d}{nFAPD_fC} \tag{3}$$

where D_s and D_f are the diffusion coefficients in the solution and film, respectively; P is the solute partition coefficient;[26] C is the redox mediator solution concentration; n is the number of electrons transferred per redox event; and F is Faraday's constant.

Equation 3 may be rearranged to give:

$$i_f^\infty = \frac{4nFrD_sC}{\left[1 + \frac{4D_sd}{\pi rPD_f}\right]} \tag{4}$$

When the SECM tip is close to a conductive substrate and the experiment is operated in "feedback" mode, the tip current is enhanced according to the equations[27]

$$i = K_G i^\infty \tag{5}$$

$$K_G = k_1 + \frac{k_2}{L} + k_3 \exp\frac{k_4}{L} \tag{6}$$

where L is the ratio of tip height above the substrate to its radius, and k_1, k_2, k_3, and k_4 are geometric factors that depend on the relative radii of the electroactive tip and its insulating sheath.[27] Since there are no redox-mediator-dependent variables in K_G, and

(25) Howell, J. O.; Wightman, R. M. *Anal. Chem.* **1984**, *56*, 524.

(26) P is defined as the ratio of solute concentrations in the film and in the solution, C_f/C.

(27) (a) Amphlett, J. L.; Denuault, G. J. *J. Phys. Chem B* **1998**, *102*, 9946. (b) Martin, R. D.; Unwin, P. R. *Anal. Chem.* **1998**, *70*, 276.

Table 1. Permeation Rates in Poly-(Fe(5-NH_2-phen)$_3^{2+}$) Films Measured Using Scanning Electrochemical Microscopy vs Rotating Disk Electrochemistry

		SECM		RDE
permeant	$D_s \times 10^6$ [a] ($cm^2\ s^{-1}$)	$PD_f \times 10^9$ (ITO)[b] ($cm^2\ s^{-1}$)	$PD_f \times 10^9$ (disk)[c] ($cm^2\ s^{-1}$)	$PD_f \times 10^9$ [d] ($cm^2\ s^{-1}$)
$Ru(NH_3)_6^{3+}$	14.5	10 ± 2	6.7 ± 0.8	11 ± 3
$Fe(CN)_6^{4-}$	7.2	18 ± 3	13 ± 3	$19 + 4$
FcMeOH	9.5	67 ± 3[e]	49 ± 5[e]	$61 + 7$
$Fe(phen)_3^{2+}$	6.1	(0.3)[f]	not determined	not detected

[a] Diffusion coefficient in solution, determined from eq 3 using limiting currents obtained at a 4.1-μm-radius carbon fiber microdisk electrode. [b] PD_f values determined from eq 4 using the slope of the plots in Figure 4A for films electropolymerized onto patterned ITO substrates. [c] PD_f values (as in (b)) from the plots in Figure 4B for films on Pt microdisk electrodes. [d] PD_f values from ref 17 determined using RDE voltammetry. [e] Value measured for oxidized permeant, $FcMeOH^{1+}$. [f] Calculated from the tip current above a 12-nm-thick polymer film (Figure 2B′); permeation current ($\ll$1 pA) was not observed for thicker films.

using the same notation as eq 5, the current at the SECM tip during positive feedback above a film-covered substrate may be written as:

$$i_f = K_G i_f^{\infty} \tag{7}$$

Combining eqs 5 and 7, if the tip geometry and its height above the substrate are constant (as in our experiments), the following is obtained:

$$\frac{i}{i_f} = \frac{K_G i^{\infty}}{K_G i_f^{\infty}} = \frac{i^{\infty}}{i_f^{\infty}} \tag{8}$$

By substituting in eqs 3 and 4

$$\frac{i}{i_f} = \frac{4nFrD_sC}{\left[\frac{4nFrD_sC}{\left(1 + \frac{4D_sd}{\pi rPD_f}\right)}\right]} \tag{9}$$

we obtain:

$$\frac{i}{i_f} = 1 + \frac{4D_sd}{\pi rPD_f} \tag{10}$$

A linear relationship between the normalized current (i/i_f) and film thickness is expected.[28]

To test eq 10, polymer films of varying thickness on the patterned ITO/photoresist substrates were prepared, but with only half of each pattern containing polymer films.[29] Using these assemblies, the SECM tip was scanned linearly at fixed height, with the substrate as generator and the tip as the collector as described above. Figure 3 shows examples of the tip current obtained during scans over patterns featuring 12- and 38-nm thick polymer films, compared with that obtained during scans over bare ITO under identical conditions. Note that the polymer film currents in Figure 3 are offset upward by 10 nA for visual illustration. Substantial attenuation of tip current occurs in scans of the film-covered versus bare ITO, a result of permeation within the polymer film. Tip currents also diminish with increasing polymer-film thickness, for example, comparing parts A and B of Figure 3, as predicted by eq 10. To quantify the relationship between SECM tip response and substrate film thickness, the amplitudes of the peak-to-peak currents in Figure 3 are taken as the background-subtracted tip current and then normalized to the response obtained over bare ITO. The line scans obtained across the surface also allow a large number of data points to be rapidly collected, so that signal averaging (which reduces the effects of

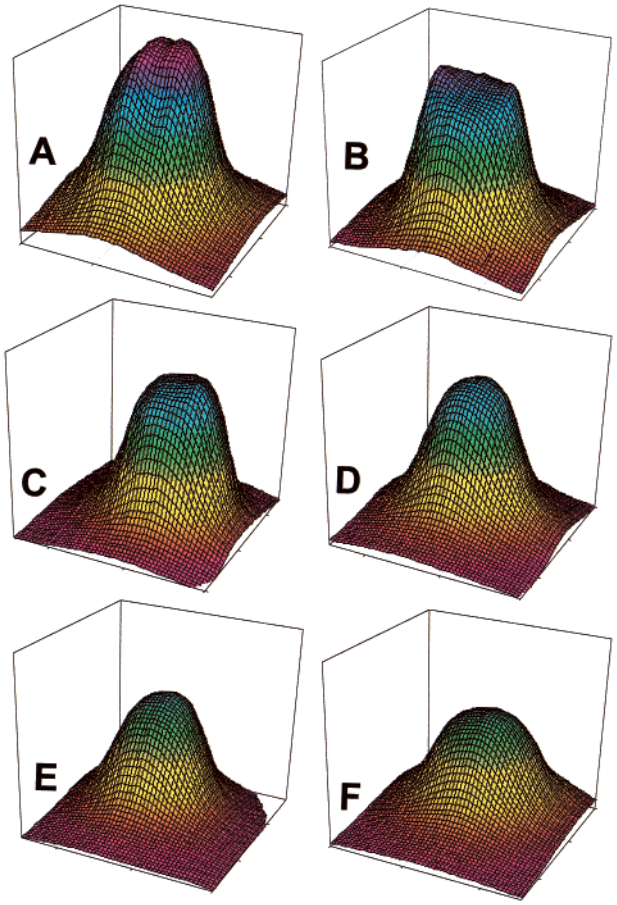

Figure 5. SECM images (40 μm $\times$ 40 μm $\times$ 2.1 nA) of 25-μm-diameter Pt disk electrodes held at +0.5 V with films that are (A) 0 nm (bare electrode); (B) 12-nm-; (C) 22-nm-; (D) 29-nm-; (E) 34-nm-; (F) 38-nm-thick. The aqueous solution contains 4.6 mM FcMeOH, and the image was taken using a 4-μm-radius carbon fiber microelectrode tip (E_{tip} = 0 V vs Ag/AgCl) at a distance of 2 μm from the Pt disk substrates, and a scan rate of 30 μm/s.

(28) This model assumes that the diffusion coefficients for the oxidized and reduced forms of the redox mediator are equivalent. Differences in transport rates based on oxidation state have been observed by SECM previously (see ref 27b) and, in the more complicated experiments here, would likely result in nonlinear terms in eq 10.

(29) Polymer films less than 10 nm thick were excluded from the study because of the anomolous permeation behavior previously observed for them. See ref 17.

differences in surface conductivity of the ITO, thickness of the photoresist, and variation in tip height) is possible.

Normalized tip currents (i/i_f) are plotted versus polymer film thickness in Figure 4A for patterned photoresist/ITO assemblies in contact with aqueous solutions of the redox mediators $Ru(NH_3)_6^{3+}$ and FcMeOH. Note that the SECM tip senses the redox reaction *product* as it diffuses from the substrate, so that the tip currents result from redox reactions of $Ru(NH_3)_6^{2+}$ and $FcMeOH^{1+}$. Each point in the plot represents the average of at least 20 data points. As expected from eq 10, the permeation current is inversely proportional to the thickness of the polymer film. Using the slopes from the linear regression of these plots, the permeabilities (PD_f) for these species have been calculated from eq 10 and are summarized in Table 1.

To further test the ability of SECM to assess permeabilities quantitatively and to confirm that the photoresist mask did not interfere with the analysis, the experiments were repeated using an assembly consisting of six coplanar Pt microdisks. Metallopolymer films of increasing thickness were sequentially electropolymerized on five of the six disk electrodes and the surface of the assembly scanned by SECM. Figure 5 shows the three-dimensional SECM images of the microdisks, taken at a 2-μm tip height in an aqueous solution of FcMeOH, where disks A−F have polymer films that are 0-, 12-, 21-, 28-, 31-, and 38-nm thick, respectively. Figure 5 demonstrates that as the polymer film thickness increases, the SECM tip current decreases: the maximum current observed in Figure 5F is ∼70% of that observed for a bare Pt disk (Figure 5A).[30] Taking the maximum current observed for each Pt microdisk and again normalizing for the bare substrate response, the ratio of the currents, i/i_f, is plotted versus polymer film thickness in Figure 5B for the permeants $Ru(NH_3)_6^{3+}$, $Fe(CN)_6^{4-}$, and FcMeOH. The values for PD_f calculated from the linear regression of these plots are given in Table 1, together with the values obtained in previous RDE experiments.[17] Comparison of the data shows that the permeation rates obtained during separate SECM and rotating-disk electrochemistry experiments are in excellent agreement.

(30) SECM images of the uncoated microdisks, which are not shown here, have tip current responses that are identical.

Finally, very small permeation tip currents are observed for thin polymer films using the redox mediator $Fe(phen)_3^{2+}$ (Figure 2B′), but are not observed for thicker (>12-nm) films. Using the permeation current from Figure 2B′ (compared with that from Figure 2B) and eq 4, a PD_f value of 3×10^{-10} cm^2/s is calculated. Permeation currents for $Fe(phen)_3^{2+}$, even for very thin metallopolymer films, were not observable by RDE,[17] highlighting the sensitivity of SECM.

CONCLUSIONS

Scanning electrochemical microscopy has been used to image size-selective permeation of redox-active species through thin polymer films. The current response of the tip over either the photoresist/ITO pattern or the Pt microdisk array is uniform, and there is no evidence of film pinholes or cracks. Further improvements in spatial resolution could well make SECM the preferred approach for evaluating permeable film morphology. PD_f values for three redox probes measured by SECM correspond well with those previously measured by RDE voltammetry, validating the SECM method as a viable and powerful analytical tool for quantitative, spatially resolved measurement of permeation rates. Future studies will focus on applying this methodology to investigate the influence of structural features (i.e., film morphology and single-crystal orientation) on molecular transport through mesoporous molecular "square" and "rectangle" materials.

ACKNOWLEDGMENT

We gratefully acknowledge the Office of Naval Research for general financial support and the National Science Foundation for a summer research fellowship for A.M.M. We thank Prof. J. B. Ketterson for use of the photolithography instrumentation, Dr. Peixing He (CH Instruments) for technical assistance with the SECM, and the reviewers for their helpful comments and suggestions.

Received for review December 21, 1999. Accepted April 26, 2000.

AC9914622